

## A New Route to Obtain Shape-Controlled Gold Nanoparticles from Au(III)- $\beta$ -diketonates

Subrata Kundu,<sup>†</sup> Anjali Pal,<sup>‡</sup> Sujit Kumar Ghosh,<sup>†</sup> Sudip Nath,<sup>†</sup> Sudipa Panigrahi,<sup>†</sup> Snigdhamayee Praharaj,<sup>†</sup> and Tarasankar Pal<sup>\*†</sup>

Departments of Chemistry and Civil Engineering, Indian Institute of Technology, Kharagpur 721302, India

Received April 12, 2004

Ligands with a  $\beta$ -diketone skeleton have been employed for the first time as reductant to produce ligand stabilized gold nanoparticles of different shapes from aqueous HAuCl<sub>4</sub> solution. Evolution of stable gold nanoparticles follows first order ( $k \approx 10^{-2} \text{ min}^{-1}$ ) kinetics with respect to Au(0) concentration. Growth of particles of different shapes (spherical or triangular or hexagonal) goes hand in hand under the influence of different  $\beta$ -diketonates, which have excellent capping and reducing properties. Chlorine insertion was observed to take place in the  $\beta$ -diketone skeleton.

Gold nanoparticles of “negligible dimension” exhibit special properties compared to those of their bulk representatives. The special properties include size- and shape-dependent optical,<sup>1</sup> electronic,<sup>2</sup> and catalytic<sup>3–6</sup> properties. These lead to their various applications such as catalysis,<sup>3–6</sup> cancer therapy, etc.<sup>7</sup> However, these particles are metastable and cannot be isolated or manipulated without appropriate stabilization by capping ligands.<sup>8</sup> Presently, a great deal of interest in the field of nanoscience is shape-selective synthesis of stabilized metal particles.<sup>9</sup> The following is the report of shape-controlled evolution and in-situ stabilization of gold nanoparticles using several well-known  $\beta$ -diketone chelating agents.

In aqueous medium, different  $\beta$ -diketonates individually serve the purpose of a ligand to generate Au(III)-chelates

which then decompose to produce isotropic Au nanoparticles. The Au nanoparticles are highly stable and possess small size with narrow size distribution, and they bear different shapes (spherical, triangular, and hexagonal). Since the method described here does not require any harsh reducing agent that might increase the local concentration of any reagent in solution during addition and it requires no manipulative skill, it is reproducible.<sup>10</sup> Although size-regime-dependent catalysis by gold particles has already been demonstrated,<sup>10</sup> the shape effect of the particles is yet to be ascertained. To the best of our knowledge, this is the first report of shape-controlled  $\beta$ -diketone stabilized gold nanoparticle synthesis out of an autodecomposition of Au(III)- $\beta$ -diketone chelates under ambient condition, with concomitant chlorine insertion in the  $\beta$ -diketone skeleton.

An aliquot of standard HAuCl<sub>4</sub> solution (final concentration  $1.8 \times 10^{-5} \text{ M}$ ) was taken in a clean beaker and was placed over a magnetic stirrer. To it, 200  $\mu\text{L}$  of aqueous  $\beta$ -diketone solution ( $\leq 10^{-2} \text{ M}$ ) was added under stirring condition at room temperature (25 °C). After several minutes of stirring, the solution turned pink because of the formation of gold nanoparticles (Supporting Information). All the spectral measurements were performed against air as reference. The absorption spectra for Au nanoparticles were recorded. The evolution of the surface plasmon band of Au<sub>n</sub><sup>0</sup> indicated the formation of gold nanoparticles. Evolution of gold particles was found to be faster when the mixture was stirred at  $\sim 60\text{--}80 \text{ }^\circ\text{C}$  on a water bath.

The UV–vis absorption spectra (Figure 1) demonstrate the evolution of gold nanoparticles from HAuCl<sub>4</sub>. The characteristic and intense absorption peak at 290 nm for aqueous HAuCl<sub>4</sub> solution can be attributed to the metal to ligand charge-transfer (MLCT) band due to the AuCl<sub>4</sub><sup>–</sup> complex.<sup>11</sup> In aqueous solution, aceoacetanilide (Aca,  $\sim 10^{-4} \text{ M}$ ) shows an absorption band with  $\lambda_{\text{max}}$  at  $\sim 240 \text{ nm}$  due to a  $\pi\text{--}\pi^*$  transition. Similarly, ethyl acetoacetate (Eaa,  $\sim 10^{-2} \text{ M}$ ), dibenzoylmethane (Dbm,  $\sim 10^{-5} \text{ M}$ ), and acetylacetone (Acac, saturated aqueous solution) in water show their  $\lambda_{\text{max}}$  values at  $\sim 248, 252, \text{ and } 270 \text{ nm}$ , respectively. Chelate

\* To whom correspondence should be addressed. E-mail: tpal@chem.iitkgp.ernet.in.

<sup>†</sup> Department of Chemistry.

<sup>‡</sup> Department of Civil Engineering.

- (1) Henglein, A. *Isr. J. Chem.* **1993**, *33*, 77–88.
- (2) Link, S.; El-Sayed, M. A. *J. Phys. Chem. B* **1999**, *103*, 8410–8426.
- (3) Pradhan, N.; Pal, A.; Pal, T. *Langmuir* **2001**, *17*, 1800–1802. Jana, N. R.; Pal, T. *Langmuir* **1999**, *15*, 3458–3463.
- (4) Jana, N. R.; Sau, T. K.; Pal, T. *J. Phys. Chem. B* **1999**, *103*, 115–121. Kundu, S.; Ghosh, S. K.; Mandal, M.; Pal, T. *New J. Chem.* **2003**, *27*, 656–662. Kundu, S.; Ghosh, S. K.; Mandal, M.; Pal, T. *New J. Chem.* **2002**, *26*, 1081–1084.
- (5) Alivisatos, A. P. *Science* **1996**, *271*, 933–937.
- (6) Lieber, C. M. *Solid State Commun.* **1998**, *107*, 607–616.
- (7) Hirsch, L. R.; Stafford, R. J.; Bankson, J. A.; Sershen, S. R.; Rivera, B.; Price, R. E.; Hazle, J. D.; Halas, N. J.; West, J. L. *Proc. Natl. Acad. Sci. U.S.A.* **2003**, *100*, 13549–13554.
- (8) Templeton, A. C.; Wuelfing, W. P.; Murray, R. W. *Acc. Chem. Res.* **2000**, *33*, 27–36.
- (9) El-Sayed, M. A. *Acc. Chem. Res.* **2001**, *34*, 257–264.

- (10) Sau, T. K.; Pal, A.; Pal, T. *J. Phys. Chem. B* **2001**, *105*, 9266–9272.
- (11) Roy Meson, W., III; Gray, H. B. *Inorg. Chem.* **1968**, *7*, 55–58.

**Table 1.** Average Size and Shape of Gold Nanoparticles from Different Au(III)- $\beta$ -diketone Chelates

name of the ligand (concentration)	average size (initial, nm) ( $\lambda_{\max}$ )	average size (final, nm) ( $\lambda_{\max}$ )	shape distribution
acetylacetonate, Acac (std aq soln)	$5.3 \pm 0.1$ (525)	$10.4 \pm 0.3$ (528)	100% spherical
acetoacetanilide, Aca ( $\sim 10^{-4}$ M)	$3.8 \pm 0.2$ (544)	$40 \pm 0.1$ (546)	$\sim 80\%$ hexagonal
ethyl acetoacetate, Eaa ( $\sim 10^{-2}$ M)	$8.8 \pm 0.1$ (548)	$27.8 \pm 0.2$ (548)	100% spherical
dibenzoylmethane, Dbm ( $\sim 10^{-5}$ M)	$3.9 \pm 0.2$ (550)	$40.4 \pm 0.1$ (550)	$\sim 90\%$ triangular

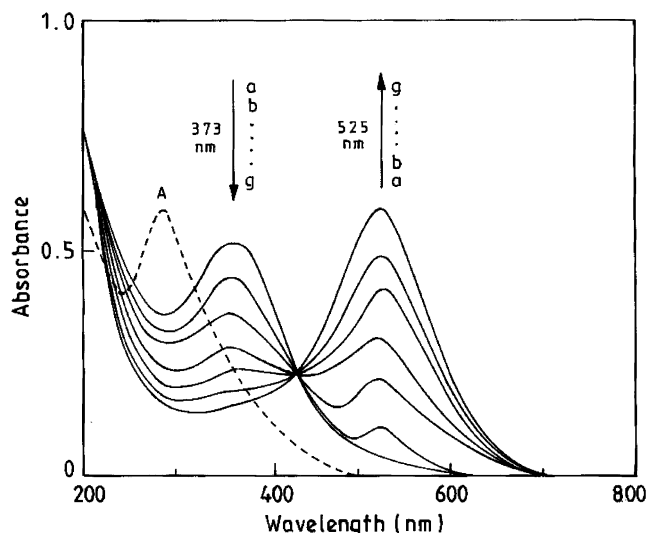


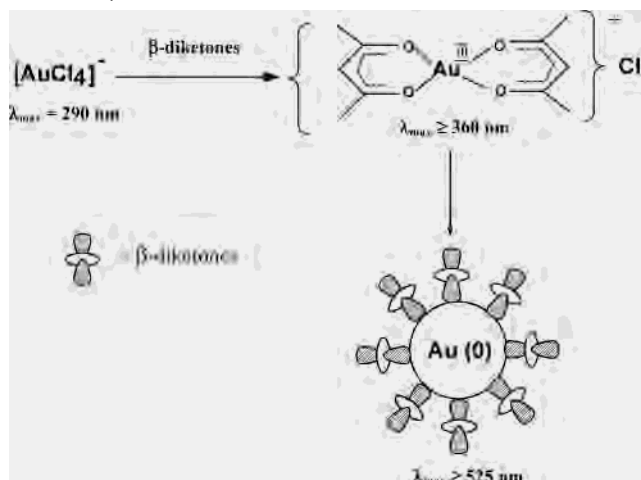
**Figure 1.** Successive evolution of plasmon bands for isotropic Au particles generated from Au(III)-Acac chelate. The dotted line with a peak at 290 nm displays the absorption spectrum of aqueous HAuCl<sub>4</sub> solution indicating a metal to ligand charge-transfer (MLCT) band. The concomitant decrease of the absorbance value at 373 nm was attributed to the decomposition of the Au(III)-Acac complex with time (a-f, 2–30 min). The successive increase of the plasmon band at 525 nm with time (a-f, 2–30 min) stands for the formation of Au nanoparticles.

formation is visualized easily from the distinct absorption bands such as 373, 376, 364, and 380 nm for Au(III)-Acac, Au(III)-Aca, Au(III)-Eaa, and Au(III)-Dbm chelates, respectively.

In Figure 1, the concomitant decrease of the absorbance value at 373 nm due to decomposition of the Au(III)-acetylacetonate chelate with successive increase of the absorbance value at 525 nm due to the formation of gold particles is shown. Similar spectral profiles for all other cases are visualized. In the case of Aca, the 376 nm peak is seen because of the Au(III)-Aca chelate and the 544 nm peak is due to formation of gold nanoparticles. For Eaa and Dbm chelates, the absorption bands appear at 364 and 380 nm, respectively, and on standing, the peaks for the evolved gold nanoparticles appear at 548 and 550 nm, respectively. Here, in all four cases, initially Au(III)-chelates are formed, and with time, these chelates decompose to produce gold nanoparticles.

Under ambient conditions, the Au(III)- $\beta$ -diketone chelates slowly decompose to evolve gold particles (Scheme 1) of variable size (10–40 nm) and shape (spherical, triangular, and hexagonal). The decomposition of Au(III)- $\beta$ -diketone can be further slowed at higher pH conditions (adding  $10^{-2}$  M NaOH) because of the removal of liberated proton as a consequence of enhanced enolization of the ligands. So, in turn the decomposition of metal chelates at higher pH takes a longer time to evolve gold nanoparticles than what is observed in normal aqueous solution at room temperature

**Scheme 1.** Schematic Presentation of Gold Nanoparticle Formation via Au(III)- $\beta$ -diketonates



(25° C). Higher pH conditions (>9.0) produce smaller gold particles. Efficient capping action of  $\beta$ -diketonates on Au surfaces and stabilization of Au particles are understood while coordinatively unsaturated surface atoms are considered. Again, the stability of Au(III) chelate as well as Au(0) particles is observed for the ligands with enhanced enolization. Enolization of the ligand increases while the ligand skeleton contains one or more aromatic rings.<sup>12</sup>

The MLCT band of AuCl<sub>4</sub><sup>-</sup> species disappears upon adding NaOH due to the formation of AuO<sub>2</sub><sup>-</sup>. Under this condition,  $\beta$ -diketonates do not show any absorption peak due to the higher concentration of OH<sup>-</sup>. Although OH<sup>-</sup> is weakly complexing with Au(III) ion, its concentration affects chelation. The level of OH<sup>-</sup> interferes with the capping ability of  $\beta$ -diketonates. In the presence of OH<sup>-</sup> (pH > 9.0), spherical, tiny Au particles are produced predominantly straightaway showing the plasmon resonance band at  $\sim 525$ –550 nm for all the cases. Even the decomposition of the gold- $\beta$ -diketonates becomes sluggish under this condition. The  $\lambda_{\max}$  value (due to gold nanoparticles) for all cases shifted toward the blue region (for Acac it shifted from 525 nm to 510 nm; for Aca, 544 to 529 nm; for Eaa, 548 to 528 nm; and for Dbm, 550 to 532 nm). The blue shift of 15–20 nm for the plasmon peak due to gold nanoparticles is observed for all the four cases even with higher ligand concentration. This shift of the plasmon peak is a qualitative signature of the formation of smaller gold particles, and this is authenticated from TEM pictures (not shown).

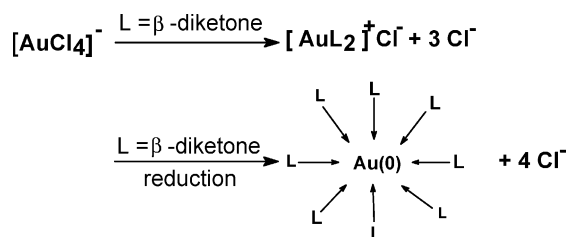
Experimentally, it has been verified that hydroxide ions play a crucial role in the reaction of Au(III) ions with  $\beta$ -diketonates. This role appears to be 2-fold:<sup>13</sup> providing the

(12) Burdett, J. L.; Rogers, M. T. *J. Am. Chem. Soc.* **1964**, *86*, 2105–2109.

necessary thermodynamic conditions that slow the reduction process and indirectly preventing the natural coalescence of smaller gold (higher surface energy) particles due to capping of the coordinatively unsaturated surface atoms.<sup>14</sup> The added NaOH abstracts the proton flanked between the two carbonyl groups, and hence, the  $\pi$ -electron cloud becomes localized which facilitates the chelation.<sup>15,16</sup> The higher stability of the chelates caused slower decomposition, and deprotonated ligands instantaneously but more efficiently cap<sup>17</sup> the evolved particles, resisting further growth of the capped particles. Deprotonation of the ligand generates  $H^+$  ions, and the resulting hydroxide ion concentration after neutralization stabilizes the Au(III) chelates. Again, it is reported that Au nucleation is pH-dependent, and higher pH conditions favor smaller particle evolution.<sup>18</sup> Ultimately, Au(III) gets reduced to Au(0). Other workers have found that simple ions direct the growth of nanoparticles into different shapes, highlighting the importance of the species.<sup>19</sup>

The evolution of gold nanoparticles was found to be first order with respect to Au particle formation, and the rate constant values were  $6.7 \times 10^{-2}$ ,  $1.4 \times 10^{-2}$ ,  $1.1 \times 10^{-2}$ , and  $0.69 \times 10^{-2} \text{ min}^{-1}$  for Acac, Aca, Eaa, and Dbm, respectively. The time of appearance of gold particles (i.e., decomposition of the chelates) with the ligands follows the order  $\text{Acac} < \text{Aca} < \text{Eaa} < \text{Dbm}$  under ambient conditions.

The evolved gold nanoparticles become capped in solution by the unreacted  $\beta$ -diketones under consideration to impart tight size distribution. Au(III) chelate formation in the presence of different  $\beta$ -diketones is studied from the conductance measurements (Supporting Information). The conductivity of aqueous  $\text{AuCl}_4^-$  increases step by step with the addition of saturated aqueous solution of  $\beta$ -diketones, and ultimately, a constant conductivity is reached. The increase in conductance is the signature for the removal of  $\text{Cl}^-$  ions from the complex  $\text{AuCl}_4^-$  species by  $\beta$ -diketones, and constancy of the conductance speaks for the completion of the chelation of Au(III) ions by  $\beta$ -diketones.



Average size, shape distribution, and absorption characteristics of gold nanoparticles obtained from different Au(III)- $\beta$ -diketone chelates are shown in Table 1. The succes-

sive red shift<sup>20</sup> is the qualitative information regarding the particle size. The shape and size distribution were confirmed from the TEM measurements indicating unidirectional growth. Representative TEMs for embryonic (a) and full-grown (b) Au particles for Acac, Aca, Eaa and Dbm case are furnished (Supporting Information). Gold sols prepared with Acac and Aca as ligand are stable for  $\sim 7$  days, and those prepared with Dbm and Eaa remained stable for months together. Nonspherical particles become better stabilized under the influence of the prescribed ligands. It was also found that during the period of particle evolution the plasmon peak positions did not alter, which reflects no further agglomeration or growth of the particles.

The enolate form of  $\beta$ -diketones (as is always the case) interacts weakly just like the compounds with amine and alcohol functionalities and preserves the electronic properties of “naked” Au(0) nanoparticles. On the other hand, thiols interact strongly with a Au surface and induce significant charge redistribution.<sup>21</sup> The observed red shift of the plasmon peak of (for  $\beta$ -diketone stabilized Au(0) nanoparticles)  $\sim 15$  nm upon addition of dodecanethiol authenticates thiol capping of the particles with the substitution of the enolate form of  $\beta$ -diketones from Au(0) surfaces.<sup>21</sup>

The reduction of Au(III)- $\beta$ -diketonates is understandable considering the strong oxidizing power of Au(III) species.<sup>22</sup> With the ligands being a reducing agent,<sup>23</sup> the reaction goes to completion, resulting in the chlorinated products. The characteristic fragmentation pattern of the products from GC-MS (Supporting Information) studies authenticates the oxidation of the ligands. The mechanism is somewhat similar to the photodecomposition of the square planar complex of Pt(II)- $\beta$ -diketonates into powder Pt(0).<sup>16</sup>

In conclusion, we present a new chemical route for the synthesis of shape selective gold particles by introducing different  $\beta$ -diketones. Here, the ligand used serves the purpose of a reducing agent, capping agent, and, hence, stabilizer. With the variation of ligand, the particle size and shape was successfully tuned. Thus, we are generalizing the new strategy for realizing ligand-stabilized shape-selective gold nanoparticles that might find wide application in nanomaterial synthesis, catalysis, and nanoelectronics.

**Acknowledgment.** We sincerely thank DST, CSIR, New Delhi, and IUC, BRNS, Mumbai, for financial support.

**Supporting Information Available:** Detailed experimental procedure containing preparation of gold nanoparticles using different  $\beta$ -diketones, conductometric study, representative transmission electron micrographs (TEMs), and brief discussion of GCMS study. This material is available free of charge via the Internet at <http://pubs.acs.org>.

IC0495214

- (13) Huang, Z.-Y.; Mills, G.; Hajek, B. *J. Phys. Chem.* **1993**, *97*, 11542–11550.  
 (14) Weitz, D. A.; Lin, M. Y. *Surf. Sci.* **1985**, *158*, 147–164.  
 (15) Lewis, F. D.; Miller, A. M.; Salvi, G. D. *Inorg. Chem.* **1995**, *34*, 3173–3181.  
 (16) Holm, R. H.; Cotton, F. A. *J. Am. Chem. Soc.* **1958**, *80*, 5658–5663.  
 (17) Han, S. W.; Joo, S. W.; Ha, T. H.; Kim, Y.; Kim, K. *J. Phys. Chem. B* **2000**, *104*, 11987–11995.  
 (18) Khan, M. A.; Peruchot, C.; Armes, S. P.; Randall, D. P. *J. Mater. Chem.* **2001**, *11*, 2363–2372.  
 (19) Filankembo, A.; Pileni, M. P. *J. Phys. Chem. B* **2000**, *104*, 5865–5868.

- (20) Fujiwara, H.; Yanagida, S.; Kamat, P. V. *J. Phys. Chem. B* **1999**, *103*, 2589–2591. Nath, S.; Ghosh, S. K.; Pal, T. *Chem. Commun.* **2004**, 966–967.  
 (21) Zhang, P.; Sham, T. K. *Phys. Rev. Lett.* **2003**, *90*, 2455021–2455024.  
 (22) Cotton, F. A.; Wilkinson, G. *Advanced Inorganic Chemistry*, 5th ed.; John Wiley & Sons: New York, 1988, p 951.  
 (23) Bhattacharjee, M. N.; Choudhuri, M. K.; Dasgupta, H. S.; Khathing, D. T. *J. Chem. Soc., Dalton Trans.* **1981**, 2587–2588.